International Journal of Nanomedicine

Dovepress

open access to scientific and medical research

Open Access Full Text Article

ORIGINAL RESEARCH

Nanoclay-Based Composite Films for Transdermal Drug Delivery: Development, Characterization, and in silico Modeling and Simulation

Muhammad Sikandar[1], Muhammad Harris Shoaib[1], Rabia Ismail Yousuf[1], Farrukh Rafiq Ahmed[1], Fatima Ramzan Ali[1,2], Muhammad Talha Saleem[1], Kamran Ahmed[1], Sana Sarfaraz[3], Sabahat Jabeen[1], Fahad Siddiqui[1], Tazeen Husain[1], Faaiza Qazi[1], Muhammad Suleman Imtiaz[1]

[1]Department of Pharmaceutics, Faculty of Pharmacy and Pharmaceutical Sciences, University of Karachi, Karachi, 75270, Pakistan; [2]Jinnah College of Pharmacy, Sohail University, Karachi, 74000, Pakistan; [3]Department of Pharmacology, Faculty of Pharmacy and Pharmaceutical Sciences, University of Karachi, Karachi, 75270, Pakistan

Correspondence: Muhammad Harris Shoaib, Department of Pharmaceutics, Faculty of Pharmacy and Pharmaceutical Sciences, University of Karachi, Karachi, 75270, Pakistan, Email harrisshoaib2000@yahoo.com; mhshoaib@uok.edu.pk

Purpose: Halloysite nanotubes (HNTs) are a versatile and highly investigated clay mineral due to their natural availability, low cost, strong mechanical strength, biocompatibility, and binding properties. The present work explores its role for retarding and controlling the drug release from the composite polymer matrix material.

Methods: For this purpose, nanocomposite films comprising propranolol HCl and different concentrations of HNTs were formulated using the "solution casting method". The menthol in a concentration of 1% w/v was used as a permeation enhancer, and its effect on release and permeation was also determined. Quality characteristics of the nanocomposite were determined, and in vitro release and permeation studies were performed using the Franz diffusion system. The data was analyzed using various mathematical models and permeation parameters. Optimized formulation was also subjected to skin irritation test, FTIR, DSC, and SEM study. Systemic absorption and disposition of propranolol HCl from the nanocomposites were predicted using the GastroPlus TCAT® model.

Results: The control in drug release rate was associated with the higher concentration of HNTs. F8 released 50% of propranolol within 8 hours (drug, HNTs ratio, 1:2). The optimized formulation (F6) with drug: HNTs (2:1), exhibited drug release 80% in 4 hours, with maximum flux of 145.812 μg/cm^{2}hr. The optimized formulation was found to be a non-irritant for skin with a shelf life of 35.46 months (28–30 °C). The in silico model predicted C_{max}, T_{max}, AUC_t, and AUC_{inf} as 32.113 ng/mL, 16.58 h, 942.34 ng/mL×h, and 1102.9 ng/mL×h, respectively.

Conclusion: The study demonstrated that HNTs could be effectively used as rate controlling agent in matrix type transdermal formulations.

Keywords: halloysite nanotube, transdermal, nanocomposite, controlled release, GastroPlus

Introduction

A pharmaceutical system that offers the passage of the drug through the skin to produce a systemic effect is termed a transdermal drug delivery system (TDDS).[1] It is one of the most promising drug conveying means due to its various advantages, such as offering continuous therapeutic effect from hours to days, avoiding frequent dosing, providing painless and easy administration, and ensuring minimal chances of toxic reactions.[2,3] These properties of TDDS provide improved patient compliance in long-term treatment especially for chronic pain and discontinuation of smoking. Therefore, a large number of TDDS are becoming commercially available day by day throughout the world.[4] However, the polymers utilized for providing controlled delivery of drug molecules from TDDS are mostly from a synthetic source, require combination with other polymers, many are claimed to be toxic, and some are expensive.[5]

Received: 29 March 2022
Accepted: 24 July 2022
Published: 4 August 2022

Halloysite nanotubes (HNTs) are nanosized clay materials consisting of nanotubes. Each nanotube is further comprised of 10 to 15 rolls of double layers (600 to 900 nm) of alumina-silica having 50 nm and 15 nm inner and outer diameters, respectively.[6] Structurally, they consist of a 1:1 ratio of tetrahedral siloxane (Si–O–Si) and octahedral aluminum hydroxide (Al–OH) layers.[6–8] The presence of the siloxane layer on the outer surface is responsible for their negative charge, while the aluminum hydroxide layer on the inner surface is responsible for their positive charge.[6] They possess significant loading and adsorption capabilities. Hence, they could interact with different molecules and help to modify their physicochemical characteristics. Moreover, their tubular structure is beneficial for improving the rheology of certain polymers and enhancing their mechanical strength.[9,10] They are considered economical with abundant natural availability, non-toxic, biocompatible, and capability of binding with the drug particles.[6–8,11] These properties make HNTs an attractive carrier for the delivery of pharmaceutical drug substances. They have been utilized successfully as a drug carrier excipient in different pharmaceutical dosage forms.[9,12,13] A slow drug release rate of more than 100 h has been achieved using the material, and their drug loading efficiency has been observed between 10% and 30%.[9] They have been utilized as nanofillers in polymers such as polyvinyl alcohol (PVA) composite to modify their physicochemical characteristics.[9] Similarly, the polymer is low-cost, biocompatible, soft, and biodegradable. It acts as a reservoir for drug substances and releases the drug as it degrades. Therefore, HNT-based composites are becoming the material of choice as a drug carrier for the development of drug delivery systems.[14] Numerous studies have been conducted for the design and characterization of HNTs/PVA-based nanocomposites.[15] The modified polymeric material has been used to improve the release profile and bioavailability of several drug substances including antihistamine, anti-inflammatory, and antibiotics.[14,16]

Propranolol hydrochloride (HCl) is a non-selective beta-blocker generally used in the management of hypertension, angina, cardiac arrhythmias, and pheochromocytoma.[17] It has a molecular weight of 259.35 g/mol, possesses a biological half-life of 2–6 h with an oral bioavailability of about 25%, and is used in an adult dose of 10–30 mg taken 3–4 times per day.[18–20] The properties of propranolol HCl, such as low molecular weight, low oral bioavailability, and short half-life, suggest that it is a potential candidate for the design of a transdermal delivery system.

In the present study, different nanocomposite films of HNT and PVA as a drug carriers were developed using a facile and convenient method for the controlled transdermal delivery of propranolol HCl (see Figure 1; diagrammatic illustration). Permeation enhancer such as menthol was incorporated in the formulations. The physicochemical characteristics were evaluated, including weight and thickness variation, folding endurance, moisture uptake, moisture content, and drug content. The release and permeation behavior of the drug from the system were determined using the Franz diffusion cell. Skin sensitivity, chemical interaction, morphology, thermal and mechanical properties were determined. In vivo characteristics were predicted using an in silico model, and stability was also determined at different temperatures.

Materials and Methods

Materials

HNTs were gifted by China Clays Ltd (New Zealand). Propranolol HCL was kindly provided by Lisko Pakistan (Private) Limited (Karachi, Pakistan), PVA was purchased from Daejung Chemicals & Metals (Gyeonggi-do, Korea), menthol from ‘Standard Scientific and Glass Works’ (Karachi, Pakistan). Potassium phosphate monobasic anhydrous from Sigma-Aldrich (St. Louis, Missouri, USA), sodium hydroxide, orthophosphoric acid, potassium dihydrogen phosphate, sodium chloride, and formaldehyde solution from Merck (Darmstadt, Germany).

Animals

Male mice (Albino) weighing 14 to 23 g used in the skin irritation test were obtained from the animal house, Faculty of Pharmacy and Pharmaceutical Sciences, University of Karachi. The study’s ethical approval was granted and approved by the Institutional Bioethics Committee (IBC) University of Karachi (Approval no: IBC KU-106/2020). All ARRIVE guidelines for the care and use of laboratory animals were followed.[21] The welfare of the laboratory animals was followed as per the guidelines of the National Research Council’s Guide for the Care and Use of Laboratory Animals.[22]

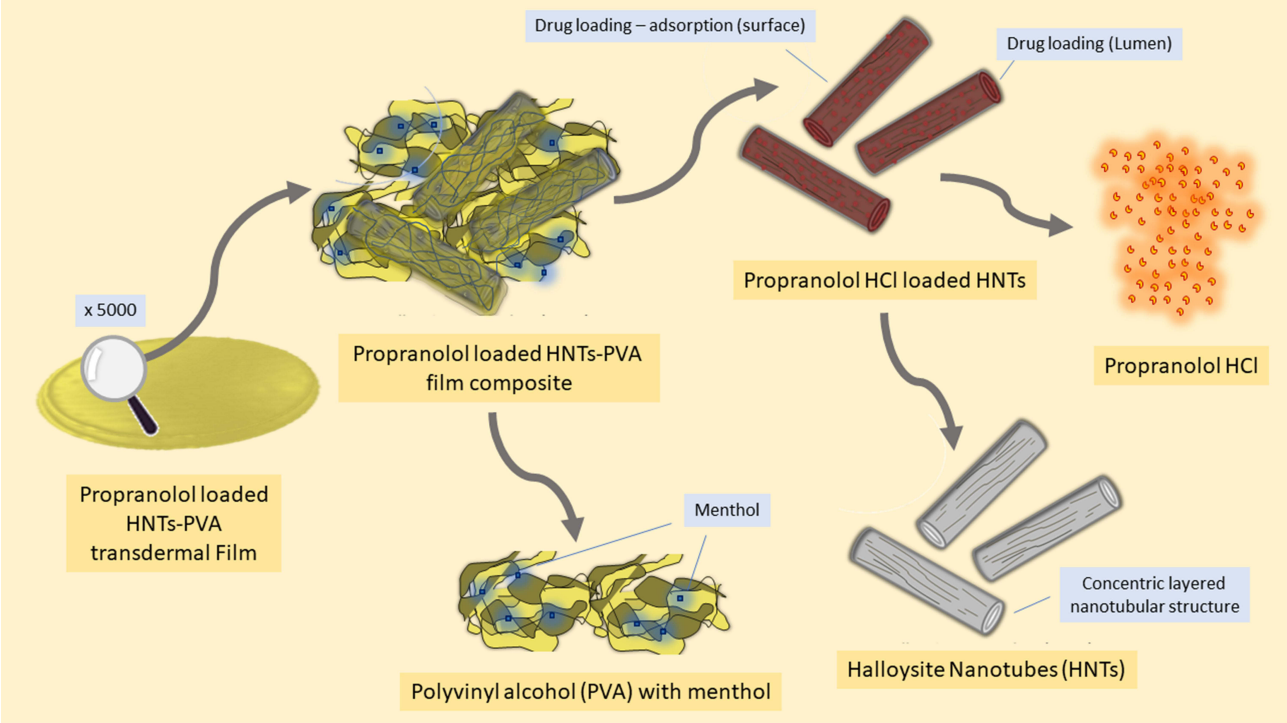

Figure 1 Diagrammatic illustrations of propranolol-loaded HNTs-PVA nanocomposite transdermal films.

Preparation of Transdermal Formulations

The formulations (containing HNTs or without HNTs) were prepared by utilizing the solvent casting method.[23] The composition of each formulation is shown in Table 1. A 2% w/v solution of propranolol HCl was prepared in deionized water. HNTs in different concentrations were incorporated in the propranolol solution with continuous agitation for 5 minutes. PVA (film former) along with or without menthol (permeation enhancer) in a fixed concentration was added in the drug and HNTs mixture, and it was agitated overnight at 250 rpm using a flat orbital shaker (KS 260 B, Industrial and Automotive Equipment, Germany). The mixture was later poured into a petri dish and dried at 60 °C for 6 hours in a hot air circulating oven (YCO-N01, Gemmy Industrial Corporation, Taiwan).

Evaluation of Formulations

Organoleptic Evaluation

The formulations were examined visually as well with the sense of touch for smoothness, flexibility, and clarity.[24]

Table 1 Composition of the Different Transdermal Composite Formulations

Formulations Code	Propranolol HCl (mg)	HNT (mg)	PVA (mg)	Menthol (mg)
F1	100	–	150	–
F2	100	–	150	50
F3	100	100	150	–
F4	100	100	150	50
F5	100	50	150	–
F6	100	50	150	50
F7	100	200	150	–
F8	100	200	150	50

Weight Variation and Thickness Evaluation

The prepared transdermal nanocomposite films (F1–F8) were subjected to uniformity of weight and thickness variation tests. For this purpose, the films, each of 1cm^2, were weighed separately on an analytical balance (Sartorius CP 224 S, Gottingen, Germany), and the readings were then recorded for performing statistical analysis. The thickness of the formulations was also determined with the help of a digital vernier caliper (Seiko Brand, China). The thickness and weight variation of the formulations were determined statistically by calculating the mean and standard deviation.[24,25]

Folding Endurance Test

The folding endurance of the formulations was determined to measure the capability of a transdermal film system to resist rupture or maintain the physical integrity with general skin folding.[26] In this test, the nanocomposite films of each formulation were repeatedly folded manually at the same place, and the number of folds required to break the film was recorded.[25,26]

Moisture Content Test

The moisture content within the nanocomposite films helps in maintaining physical stability. The moisture content of formulations was determined by weighing each film and keeping it in a desiccator (containing silica gel as a desiccant) at normal room temperature. Their weight was measured after every 24 hours until a constant weight was attained. The percentage moisture content was calculated by using equation 1.[27]

$$\%\ \text{Moisture content} = \frac{\textit{initial weight of the film} - \textit{final weight of the film}}{\textit{initial weight of the film}} \text{x } 100 \quad (1)$$

Moisture Uptake Test

The capability of a polymeric nanocomposite film to uptake moisture content from the environment is considered to affect the release rate of the drug from the system.[28] The formulations were subjected to moisture uptake test by weighing each film initially and keeping it in a desiccator containing a saturated solution of sodium chloride. The weight of each film was measured after every 24 hours until a constant weight was achieved. Equation 2 was used to calculate the percentage moisture uptake.[29]

$$\%\ \text{Moisture uptake} = \left(\frac{\textit{final weight of the film} - \textit{initial weight of the film}}{\textit{initial weight of the film}}\right) \text{x } 100 \quad (2)$$

Content Uniformity

All the nanocomposite formulations (F1-F8) were subjected to content uniformity test for determining the percent amount of drug in the formulation. The content of the drug in each formulation was determined by following the HPLC technique as described in British Pharmacopoeia (BP 2020). The chromatographic separation was performed by using High-Pressure Liquid Chromatograph (LC-20A Shimadzu, Kyoto, Japan). The mobile phase (100 mL) was prepared by mixing 1 mL aqueous sulfuric acid (10% v/v), 2 mL of *tetra*-butylammonium dihydrogen orthophosphate (1.7% w/v), acetonitrile (60% v/v), sodium dodecyl sulphate (0.115% w/v) and 37% v/v distilled water. The mobile phase was pumped (isocratic) at a rate of 1.8mL/min through a C18 column (20 × 4.6cm, Mediterranean Sea 5µm) maintained at an ambient temperature by a column oven (CTO-20 A, Shimadzu, Kyoto, Japan). The peak response of propranolol HCl was recorded at 289 nm using a UV detector (SPD-20A, Shimadzu, Kyoto, Japan).

The standard solution was prepared in a 100 mL volumetric flask by dissolving 3.33 mg of propranolol HCl in phosphate buffer B.P. having a pH of 7.4. Similarly, the test solution was prepared by dissolving a 1cm^2-sized film in the same buffer solution. The solution was agitated overnight on a flat orbital shaker at a speed of 250 rpm and sonicated using Elmasonic D-78224 (Elma, Germany) for 15 minutes.

In vitro Drug Release Study

The release rate of the drug from the nanocomposite films was determined by using Franz Diffusion Cell (V9-CB Manual diffusion system, PermeGear Incorporated, USA). A film of 1 cm^2 size was selected from each formulation.

A fiber net of appropriate size carrying the transdermal formulation was placed between the donor and acceptor compartment. The acceptor compartment was loaded with 5 mL of phosphate buffer B.P., having a pH of 7.4. The temperature of the water jacket was held at 37 °C.[29] And, 0.5 mL aliquots of the drug samples were collected in triplicate at different time intervals (0, 5, 10, 15, 30 min, and 1, 2, 3, 4, 5, 6, and 8 h) and diluted separately with an appropriate volume of the phosphate buffer. The drug concentration in each sample was determined by using a double beam UV-Vis. Spectrophotometer (UV-1800, Shimadzu Corporation, Kyoto, Japan) at a wavelength of 289 nm. The drug release kinetics was determined by using different drug release kinetic models such as zero order, first order, Higuchi, and Korsmeyer–Peppas (Equation 3–6) using the Microsoft Excel add-in program DDSolver.[30]

$$Q_1 = Q_0 + K_0 t \tag{3}$$

where $Q_{1\ \text{and}}\ Q_0$ are the amounts of drug dissolved at a particular time t and the amount of the drug present at time zero in the dissolution media, and K_0 is the zero-order rate constant.

$$log\ Q_1 = log\ Q_0 + \frac{K_1 t}{2.303} \tag{4}$$

where $Q_{1\ \text{and}}\ Q_0$ are the amounts of the drug in the dissolution media at time t and zero, and K_1 is the first-order rate constant.

$$Q_t = K_H t^{1/2} \tag{5}$$

where Q_1 is the dissolved amount of the drug in the dissolution media at time t, $t^{1/2}$ is the square root of time (t), and K_{H} is the rate constant for the Higuchi model.

$$Q_t = at^n \tag{6}$$

where a is a constant that depends on geometric and structural characteristics of the dosage form and n is the release exponent indicating the mechanism of drug release.

In vitro Permeation Study

The permeation test was conducted by Franz Diffusion Cell using dialysis tubing (500 g/mol cut-off molecular weight) as a barrier membrane.[31] Sample nanocomposite films of 1 cm^2 size were placed between the donor and acceptor compartment. The acceptor compartment was filled with 5 mL of phosphate buffer pH 7.4. The temperature of the water jacket was held at 37 °C.[32] And, 0.5mL aliquots of the drug samples were collected in triplicate at a different time intervals (0, 0.25, 0.5, 1, 2, 4, 6, 8, 10, and 12 h) and diluted with an appropriate volume of the same buffer. The absorbance of the drug in each sample was determined by a UV-Vis spectrophotometer (UV-1800, Shimadzu, Japan) at a wavelength of 289 nm, and the amount of the drug diffused through the barrier membrane at different time intervals was calculated. Permeation profiles were obtained by plotting a graph between the amount of drug permeated (μg/cm^2) versus time. Various permeation parameters such as flux, permeation coefficient, lag time, and diffusion coefficient were also determined using the method stated by Ubaidulla in 2007.[33] The flux (J) was calculated as the slope of the graph plotted between the linear portion of the cumulative amount of drug permeated and time. Whereas the lag time (L) was determined by extrapolating the line of the same graph to the abscissa. The partition coefficient (P) and the diffusion coefficient (D) were calculated by using equations 7 and 8.[34,35]

$$P = \frac{J}{C_d} \tag{7}$$

where P is the partition coefficient, J is the flux and C_{d} is the amount of drug in the donor compartment.

$$D = \frac{h^2}{6L} \tag{8}$$

where D is the diffusion coefficient, h is the thickness of the membrane and L is the lag time.

Fourier Transform Infrared (FTIR) Spectroscopy

The compatibility of the drug with the excipients in the optimized formulation was determined by FTIR spectroscopy (Nicolet Avatar 330, ThermoFisher Scientific, USA) study. The raw FTIR data of the was used to construct a composite plot in MS Excel 365 for all the samples, whereas the images generated from the OMNIC software ver. 7.3 (ThermoFisher Scientific, USA) are presented in Figures S1 and S2. The obtained spectra were compared for any chemical incompatibility of the samples with the drug present in the composite transdermal film.

Differential Scanning Calorimetry (DSC)

The thermal behavior of propranolol HCl, PVA, HNT, PVA/HNT nanocomposite film and the optimized formulation were determined using DSC (DSC 250, TA Instruments, DE, USA) method to study the mechanical properties of the samples. The heating of the samples was carried out at a rate of 10 °C/min in a temperature range of 30 to 240 °C. The raw data of the thermogram were used to construct a composite plot using MS Excel 365 for all the samples, whereas the images generated from the TRIOS software (TA Instruments, New Castle, DE, USA) are presented in the Figures S1 and S2. The obtained thermograms were compared for any change in thermal and mechanical properties of the samples in the composite transdermal film.

Scanning Electron Microscopic (SEM) Analysis

The surface morphology of the prepared transdermal polymeric films with or without HNTs was analyzed by scanning electron microscope (SEM, JEOL JSM 6380-A, Tokyo, Japan) at an accelerating voltage of 20 kV. Sputter coating of the samples was carried out with gold up to 250°A using an automated sputter coater (JEOL FC-1500). The images obtained were compared for the difference in surface characteristics between the films.

Skin Irritation Test

The optimized nanocomposite transdermal film formulation (F6) was subjected to skin irritation test, using mice as subjects. Six mice were taken. The animals were kept at normal room temperature with free access to food and water. The National Research Council and the ARRIVE guidelines for the use and care of laboratory animals were properly followed.[21,36] A particular area of the skin was shaved using an electric hair clipper (KM-6330, Kemei, China) a day before the test. The optimized formulation was applied on three of the animals (marked as test) on the area with the help of CoTran 9697 Tape (3M, Saint Paul, USA) for 24 hours. It was then evaluated for any signs and symptoms of edema or erythema. In addition, an aqueous solution of 0.8% formalin was applied on the remaining three animals (marked as control).[37] The site of applications was rated based on the method described earlier by Vlasses et al 1985.[38]

In silico Modeling and Simulation

The systemic disposition of propranolol HCl from optimized transdermal nanocomposite film was predicted using the "Transdermal Compartmental Absorption and Transit" (TCAT®) model embedded in GastroPlus™ software version 9.8 (Simulations Plus Inc., Lancaster, CA, USA). Several formulations, physiological and pharmacokinetic parameters obtained from the literature,[17,18,39–41] and ADMET™ predictor (in GastroPlus™) module were incorporated as shown in Table 2. The simulation was performed using 'transdermal: reservoir patches' as dosage form under human-fed conditions and the human arm was selected as the dosing application region. Diffusivity values in various layers of skin were used as predicted by the default in silico method present in GastroPlus®. The pharmacokinetic parametric values of propranolol HCl were calculated after processing and modeling (compartmental modeling) the reported in vivo pharmacokinetics data of extended-release (ER) propranolol HCl 80 mg tablets in the PKPlus™ module of GastroPlus™.[42] The predicted plasma profiles obtained from single and multiple doses of propranolol HCl were cross-matched with the reported in vivo profile and various pharmacokinetic parameters of optimized formulation were compared.

Stability Study

The stability study of the optimized nanocomposite film formulation (F6) was conducted according to the method reported by Puri et al.[43] In the stability testing, the samples of the optimized formulation packed separately in an

Table 2 Formulation, Physiological and Pharmacokinetic Input Parameters Used for the Development of PBPK Model of Propranolol HCl Using GastroPlus™

Parameter	Value	Source
Log P	3.03	Calatayud-Pascual et al, 2018[18]
pKa	9.45	Information, N.C.f.B., 2022[19]
Molecular weight (*MW*) (g/mol)	259.35	ADMET Predictor™
Aqueous solubility (*S*) (mg/mL)	0.0617	Drug Bank 2022[40]
Dosage form	TD: Reservoir Patch	Adjusted
Dosing region	Arm	Adjusted
Application surface area (cm^2)	9	Adjusted
Jejunal effective permeability (P_{eff}) (cm/sec $\times 10^{-4}$)	2.5	ADMET Predictor™
Unbound percent in human plasma (% F_{up})	10	Al-Majed et al, 2017[17]
Human blood to plasma concentration ratio (R_{bp})	0.89	Taylor and Turner., 1981[41]
Stratum corneum diffusivity (cm^2/s)	2.259×10^{-11}	TCAT® model
Epidermis diffusivity (cm^2/s)	1.857×10^{-6}	TCAT® model
Dermis diffusivity (cm^2/s)	4.45×10^{-6}	Calculated from in vitro permeation data
$t_{1/2}$ (h)	10.2	PKPlus™
V_c (L/kg)	3.11	PKPlus™
Clearance (C_L) (L/h)	14.79	PKPlus™

aluminum foil were placed in a stability chamber (NuAire, Plymouth, MN, USA) at 28–30°C (room temperature) and 40–45°C (accelerated temperature) for 3 months. The samples were not only evaluated physically but the drug content, drug release and permeation rate were also determined at different time intervals. The shelf life was also calculated by using Minitab Statistical Software version 20.2, 2021.

Result and Discussion

Organoleptic Evaluation

The transdermal nanocomposite film formulations were physically examined to determine texture, flexibility and clarity. All the formulations were found to possess satisfying clarity, texture and brittleness as shown in Table 3. An inverse relation was found between the concentration of HNTs and the film's clarity and smoothness. The formulations without HNTs (F1 and F2) were found to have the greatest smoothness and clarity. The smoothness and clarity of formulations were observed to decrease with an increase in the proportion of HNTs. The formulations F3 and F4 were found to have

Table 3 Physical Appearance of Transdermal Films

Formulations	Smoothness	Clarity	Flexibility (Non-Brittleness)
F1	++++	++++	++++
F2	++++	++++	++++
F3	++	++	++++
F4	++	++	++++
F5	+++	+++	++++
F6	+++	+++	++++
F7	+	+	++++
F8	+	+	++++

Note: Levels of satisfaction: Excellent = ++++, Good = +++, Fair = ++, Passable = +.

a greater smoothness and clarity than F5 and F6. In comparison, the formulations with the highest concentration of HNTs (F7 and F8) were found to have a rough texture.

Weight Variation and Thickness Variation

The mean weight and thickness of the nanocomposite film formulations were calculated along with the standard deviation. The results shown in Table 4 indicate that both the weight and thickness of all formulations did not deviate vastly from their mean value. A low SD value and closeness of results among the films of the same formulation indicate uniformity.[44] Furthermore, it was also noticed that as the concentration of HTNs was increased in the formulations, the weight and thickness were also enhanced.

Folding Endurance

The folding endurance test determined the flexibility and physical stability of all the transdermal film formulations, as shown in Table 4. The value of folding endurance (>300-fold) indicates that all the formulations can withstand the skin's folding and retain its physical stability.[26]

Moisture Content

The results of the moisture content are shown in Table 4. The results indicated the highest moisture content in formulations without HNTs (F1 and F2). Moisture content was found to decrease with an increment in HNTs amount (F3–F8). High moisture content in the polymer was supposed to be due to the hydrophilic nature of the compound.[27] The presence of SiO_2 and a small number of hydroxyl groups in HNTs make the clay hydrophobic, resulting in strong hydrogen bonding with polymer matrices and reducing the interaction of the composite with water molecules.[45]

Moisture Uptake

The average percent moisture uptake by the nanocomposite film formulations is shown in Table 4. It was observed that moisture uptake capability was increased with a reduction of HNTs amount in the formulations. Low moisture content in the formulation is considered favorable as it reduces the chances of microbial contamination and enhances stability.[46]

In vitro Drug Release Study

The in vitro drug release profiles of the nanocomposite film formulations are presented in Figure 2. The dissolution profile of formulations indicated an initial burst effect within 10 minutes. The burst effect of the drug from the formulations was supposed to occur due to the presence of adsorbed drug molecules on the outer surface of the HNTs.[47] The dissolution rate of the drug in formulations without HNTs (F1 and F2) was the highest (>80% drug was

Table 4 Quality Characteristics and Drug Content Uniformity of Propranolol HCl Nanocomposites

Formulations Code	Weight (mg) ± S.D.	Thickness (mm) ± S.D.	Folding Endurance	Moisture Content (%) ± S.D.	Moisture Uptake (%) ± S.D.	Drug Content (%/cm^2) ± S.D.
F1	7.833±0.057	0.17±0.01	>300	4.952±0.522	14.014±2.104	98.213±0.25
F2	9.633±0.208	0.223±0.011	>300	4.497±0.575	11.266±2.484	92.843±0.35
F3	10.866±0.057	0.253±0.005	>300	1.567±0.703	10.664±1.513	90.404±0.433
F4	12.633±0.057	0.296±0.015	>300	1.226±0.527	9.784±0.856	91.52±0.604
F5	9.733±0.057	0.213±0.005	>300	2.394±0.576	11.929±1.215	100±1.027
F6	10.767±0.057	0.243±0.005	>300	2.553±0.018	9.609±0.796	96.423±0.314
F7	14.566±0.152	0.326±0.005	>300	0.455±0.394	9.194±0.343	90.819±0.723
F8	15.733±0.057	0.393±0.005	>300	0.635±0.002	6.524±0.96	90.612±0.661

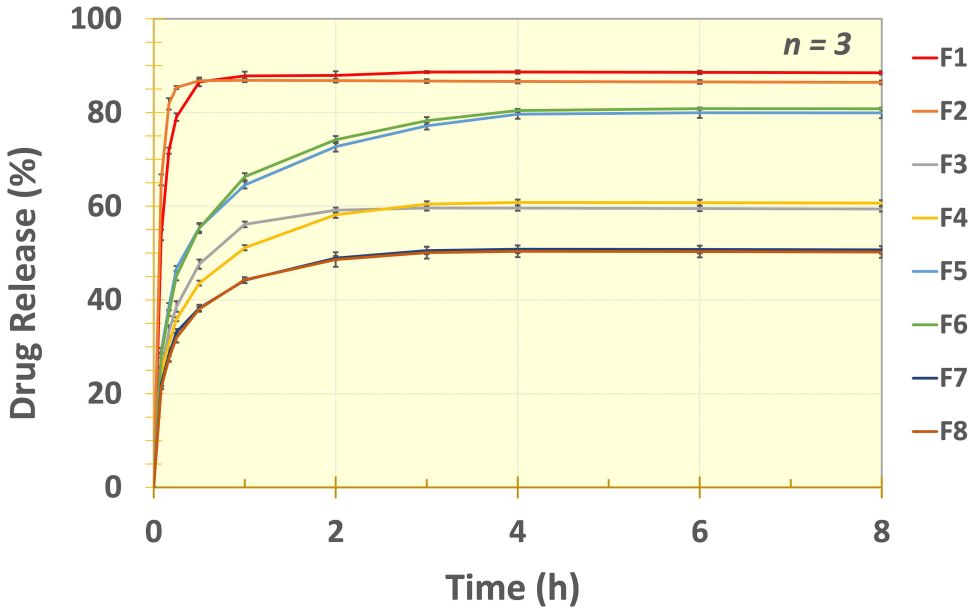

Figure 2 The in vitro release profile of propranolol HCl transdermal nanocomposite film formulations (F1–F8).

released in 30 min) among all. A rapid drug release from the formulations was observed due to the presence of hydrophilic polymer prepared without HNTs.[48] The formulations (F3 and F4) containing drug and HNTs in the same amount (1:1) showed about 60% drug release in 8 h (480 min). The nanocomposite films (F5 and F6) containing drug and HNTs in a ratio of 2:1 showed about 80% drug release in the first 4 h (240 min). About 50% of the drug was released from the transdermal films (F7 and F8) containing drug and HNTs in a ratio of 1:2 within 8 h (480 min). However, a desired controlled release profile of propranolol HCl was obtained by using drug and HNTs in a ratio of 2:1 (F6). In a study conducted by Levis and Deasy, a similar sustained released effect of propranolol HCl was observed from the halloysite nanotubes, and about 80% of the drug was released in 8 h.[49]

These release profiles indicated that with an increment of HNTs ratio in the transdermal films, the drug release rate was retarded. Levis and Deasy in 2003 reported that the release rate of propranolol HCl was observed to decrease by loading into halloysite and increasing the concentration of halloysite in the formulation. A similar inverse relationship of HNTs' concentration with drug release was also reported by many researchers.[8,50] The decrease in drug release rate in the presence of HNTs is considered due to loading of drug into the material lumen or strong ion interaction between drug and HNTs as well as improvement in mechanical properties and enhancement in the thermal stability of the polymer composite.[8,15,51]

The dissolution data of the formulations were subjected to different release kinetic models, including zero order, first order, Higuchi, and Korsmeyer–Peppas, and the results are presented in Table 5. Korsmeyer–Peppas model was best fitted in the dissolution data with an r^2 value of 0.9655 to 0.9835. The n values of the formulations were less than 0.5, representing Fickian diffusion as the drug release mechanism.[52] The same model was observed fitted by Abdouss et al, where HNT-methionine nanocomposite was formulated for the controlled delivery of phenytoin, and by Mohebali et al, where HNT/PVA nanocomposite was developed for the controlled delivery of minocycline.[47,53] The Korsmeyer–Peppas release constant (K_{KP}) value was highest in formulations without HNTs (F1 and F2). The K_{KP} was found to decrease proportionally with an increase in the amount of HNTs.[54] The dissolution profile of optimized formulation (F6) after the Korsmeyer–Peppas model (r^2 = 0.979) was found to best fit in the first-order release model (r^2 = 0.979), indicating concentration-dependent drug release.

Table 5 Mathematical Modeling and Comparison of Propranolol HCl Release Profile from the Formulations

Mathematical Models	Parameters	F1	F2	F3	F4	F5	F6	F7	F8
Zero-order	K_o (conc.mint.$^{-1}$)	0.282	0.276	0.187	0.189	0.246	0.249	0.159	0.157
	r^2	0.4588	0.3583	0.6328	0.6963	0.7235	0.7261	0.6648	0.6660
First-order	K_1 (mint.$^{-1}$)	0.125	0.181	0.005	0.005	0.026	0.026	0.003	0.003
	r^2	0.9883	0.9835	0.7724	0.8276	0.9631	0.9707	0.7524	0.7531
Higuchi	K_H (mint.$^{-1/2}$)	5.968	5.916	3.871	3.866	5.003	5.056	3.263	3.234
	r^2	0.6317	0.5241	0.8013	0.8526	0.8719	0.8751	0.8258	0.8277
Korsmeyer–Peppas	K_{KP} (mint.$^{-n}$)	61.299	73.288	26.090	22.900	27.767	26.968	21.538	20.924
	n	0.069	0.032	0.150	0.174	0.186	0.193	0.153	0.157
	r^2	0.9713	0.9835	0.9655	0.9786	0.9821	0.9790	0.9792	0.9767

In vitro Permeation Study

The permeation profile of all the transdermal film formulations is presented in Figure 3 along with permeation parameters as shown in Table 6. The amount of permeation per unit area was found to be improved with the incorporation of HNT. However, the flux of the drug from the formulations was found to be inversely proportional to the amount of HNTs in the formulation. Furthermore, the rate of permeation was observed improved in the formulations (F2, F4, F6, F8) containing menthol with a flux of 56.819 µg/cm^{2}hr, 103.225 µg/cm^{2}hr, 145.812 µg/cm^{2}hr, and 87.724 µg/cm^{2}hr as compared to the formulations (F1, F3, F5, F7) without menthol with a flux of 33.021 µg/cm^{2}hr, 85.763 µg/cm^{2}hr, 128.080 µg/cm^{2}hr and 78.484 µg/cm^{2}hr respectively. It has been reported that menthol in a concentration of 1% w/v is a suitable permeation enhancer. It is believed that terpenes such as menthol form permeable boundary regions that enhance the drug permeation rate from the formulation. In one of the reported studies, Jeevan et al observed a flux of 122 µg/cm^{2}hr.[55]

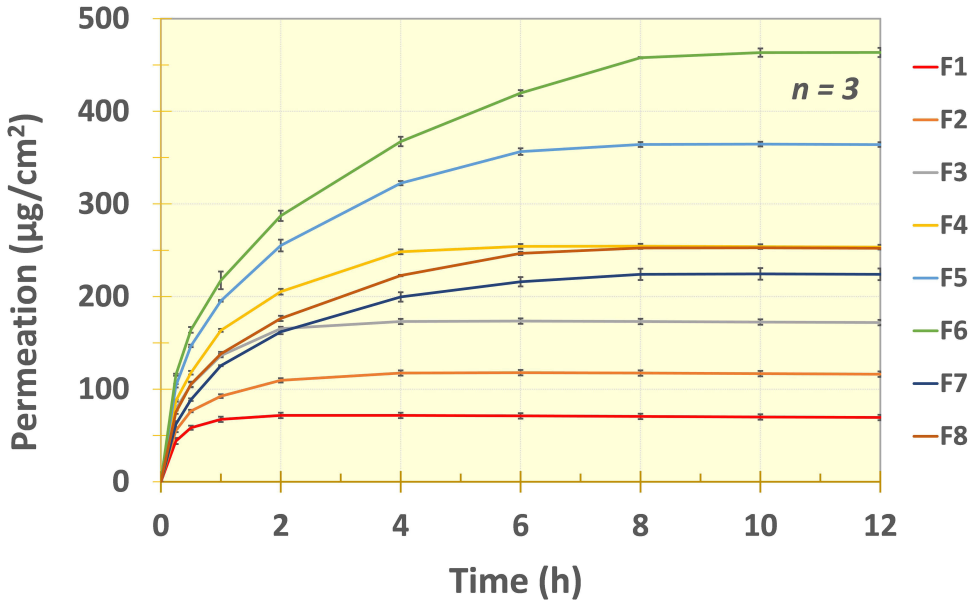

Figure 3 The in vitro permeation profile of propranolol HCl transdermal nanocomposite film formulations (F1–F8).

Table 6 Permeation Parameters of Propranolol HCl Transdermal Nanocomposites

Formulations	Flux (J)	Permeability Coefficient (P_C)	Lag Time (t_{lag})	Diffusion Coefficient (D)
	μg/cm^{2}hr	cm/hr	hr	cm^2/hr
F1	33.021	0.050	0.644	2.329E-06
F2	56.819	0.086	0.386	3.88E-06
F3	85.763	0.129	0.341	4.39E-06
F4	103.225	0.156	0.336	4.45E-06
F5	128.080	0.194	0.339	4.42E-06
F6	145.812	0.220	0.336	4.45E-06
F7	78.484	0.118	0.353	4.24E-06
F8	87.724	0.132	0.371	4.04E-06

The permeation rate of propranolol HCl was observed slowest from the film formulation (F1) without HNTs. The formulation F6 containing drug and HNTs in a ratio of 2:1 showed the highest amount (about 463 μg/cm^2) of propranolol HCl permeated per unit square within 12 hours. In a study by Krishna and Pandit, about 1248 μg/cm^2 propranolol was permeated in 24 hours from the optimized patch of size 2.5 cm^2.[56] An increase in the amount of drug permeation with a reduction in the ratio of HNTs can be related to a faster dissolution rate of the drug. This results in a more significant amount of drug available at the site of permeation and that too in the presence of menthol. It has been revealed that the nanotubes also enhance the permeation rate of the drug molecules. This might be due to the nano-size structure of the HNTs, enhancing the penetration power of the drug molecules across the barrier membrane.[7,57] Similarly, the highest lag time was observed from the formulation (F1) without HNTs or the permeation enhancer, while the lag time was found reduced in the presence of the permeation enhancer or HNTs. Whereas, the lowest lag time was observed from the formulation F6, 0.336 h among the all. Similarly, a lag time of 0.50 h was observed by Jeevan et al. They reported a decrease in the lag time of propranolol in the presence of menthol.[55]

Based on the above results, film formulation, F6, was selected as the optimized formulation. It was therefore further evaluated for skin irritation, chemical interaction, surface morphology and stability.

Drug Content

The content uniformity test results of all the transdermal formulations are given in Table 4. The results indicated that the mean amount of drug in all formulations was within a limit of 90–100%. The propranolol HCl content in the F6 was found to be 94.60% ± 1.74% (see Figure 4), meeting the official compendia limit (90.0–110.0%) for the drug content.[58]

Fourier Transform Infrared (FTIR) Spectroscopy

The FTIR spectra of the film (containing the propranolol HCl, HNTs, PVA, and menthol) and pure propranolol HCl were recorded at 4000 to 400 cm^{-1} scanning range. The spectra results were then compared (see Figure 5 and Figure S1). The spectra of propranolol HCl showed naphthalene stretch at 796 cm^{-1}, O–CH bond stretch at 1240 cm^{-1}, C=C stretching at 1579 cm^{-1}, C–H bending at 2983 cm^{-1} and O–H bending vibrations at 3691 cm^{-1}.[59] The equivalent FTIR peaks in the formulated film were at 796 cm^{-1}, 1240 cm^{-1}, 1579 cm^{-1}, 2921 cm^{-1} and 3676 cm^{-1}. A slight change in bending vibration at 2983 cm^{-1} and 3691 cm^{-1} was observed. It might be due to the C–H bond of PVA and O–H group present at HNTs' surface.[51,60] It can be concluded that there is no chemical interaction between the film components.

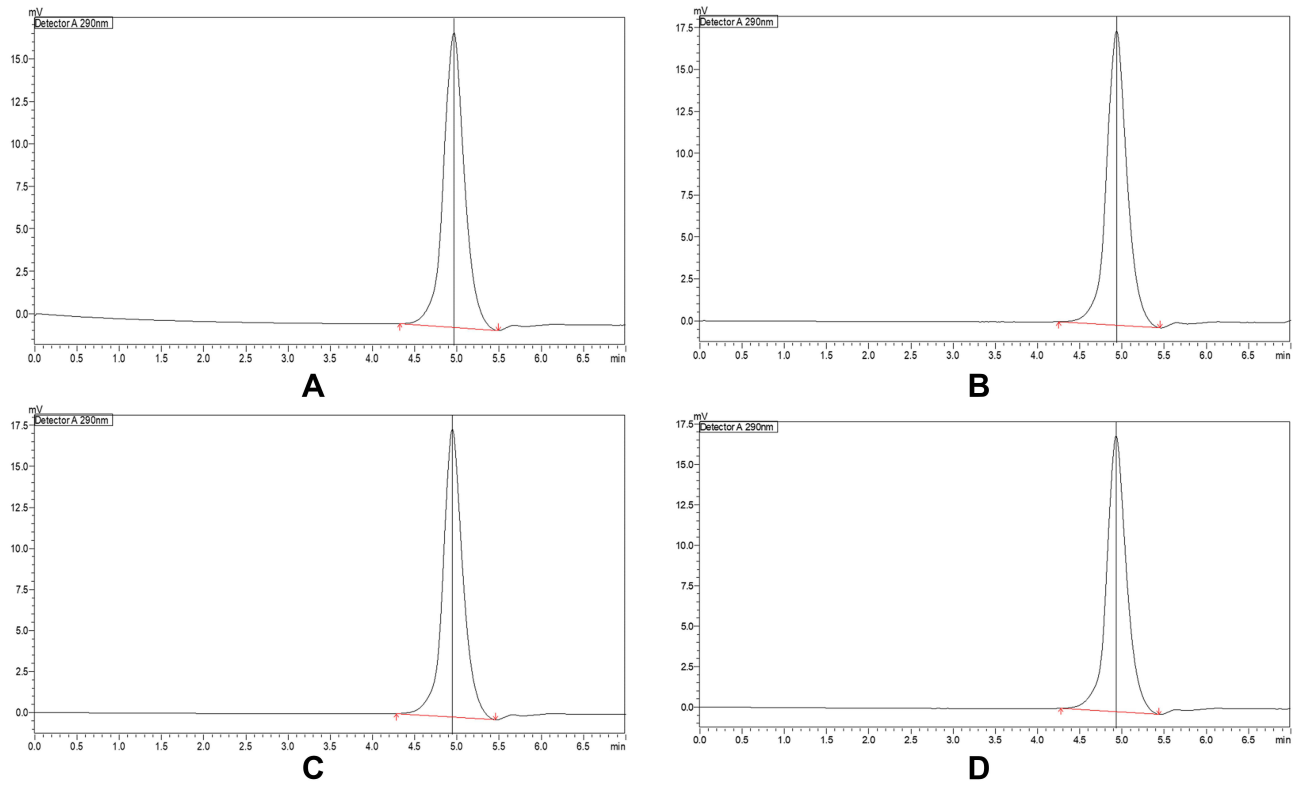

Figure 4 HPLC-UV chromatogram of propranolol HCl (**A** and **B**) and transdermal nanocomposite formulation F6 (**C** and **D**).

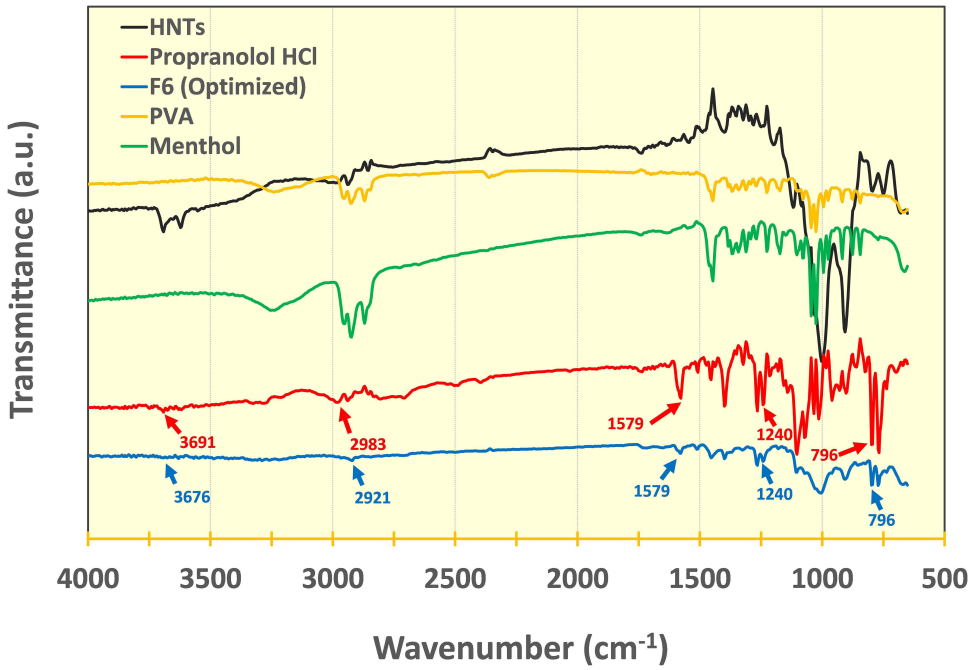

Figure 5 FTIR spectrum of the propranolol HCl, HNT's, PVA, methanol and transdermal nanocomposite formulation F6.

Differential Scanning Calorimetry (DSC)

The DSC plots of propranolol HCl, PVA, HNT, PVA/HNT nanocomposite and the optimized formulation F6 are presented in Figure 6 and Figure S2). Halloysite nanotubes have a very stable structure, and apart from the removal

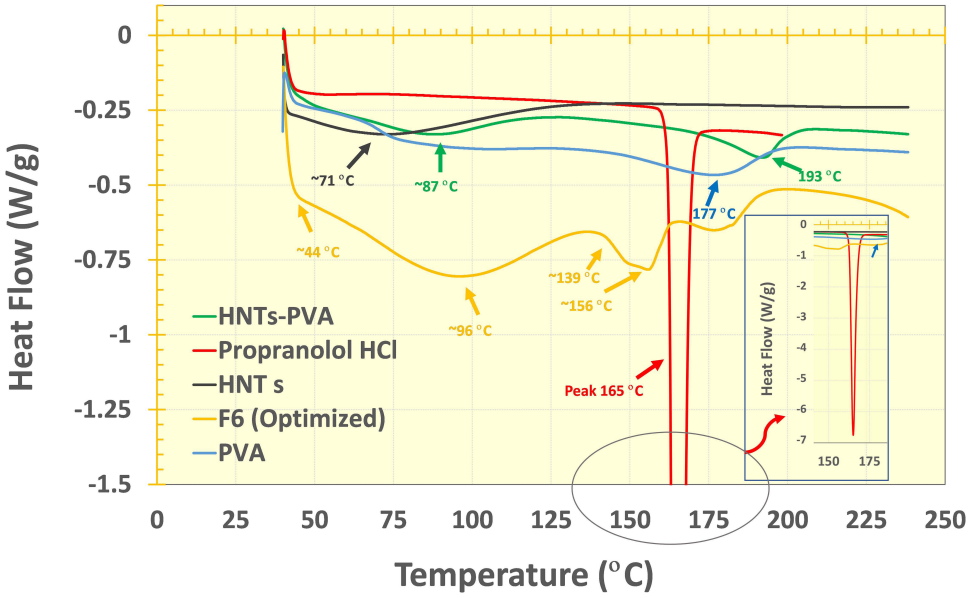

Figure 6 Thermograms, representing thermal transitions, of (**A**) propranolol HCl (**B**) HNT (**C**) PVA (**D**) PVA/HNT nanocomposite film and (**E**) optimized formulation F6.

of surface and intercalated moisture, which is evident by a broad endothermic event from ~45–140 °C, there is no other thermal phenomenon observed.[61] Since PVA is a partially crystalline polymer with varying levels of hydrogen bonding with the surface –OH groups of nanotubes, the characteristic endothermic phenomena (~173 °C) were found to shift to higher temperature values in the HNT-PVA composites.[15] In the case of optimized formulation (F6), however, the sharp endothermic drop at ~44 °C is attributed to the melting of menthol in a small amount in the formulation (permeation enhancer 1%) along with its thermal oxidation at around ~138–150 °C.[62] This thermal event in the F6 (optimized formulation) is fused with the melting of the propranolol HCl in the formulation, which would be present in the amorphous form as reported for various drugs loaded onto HNTs and propranolol HCl adsorption on clays.[63–65] Moreover, the melting of the drug was followed by volatilization at around ~179 °C.[63] As confirmed by the FTIR and HPLC analysis, the drug was found chemically stable in the films. The composite's high mechanical and thermal stability is largely responsible for slow release of the drug for the formulation.[23,66]

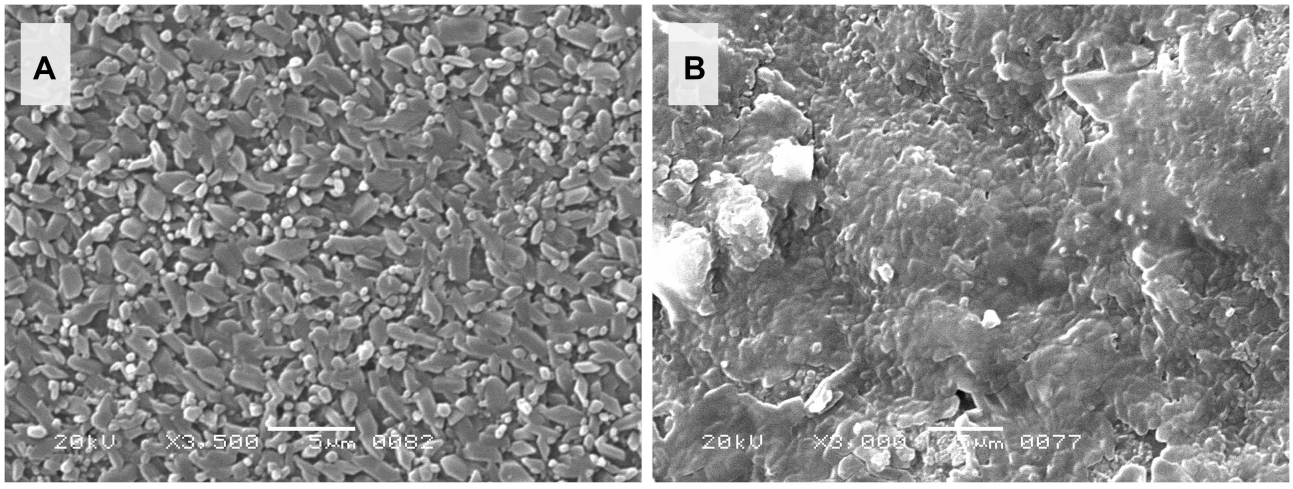

Figure 7 SEM image of PVA film (**A**) without HNTs and (**B**) with HNTs.

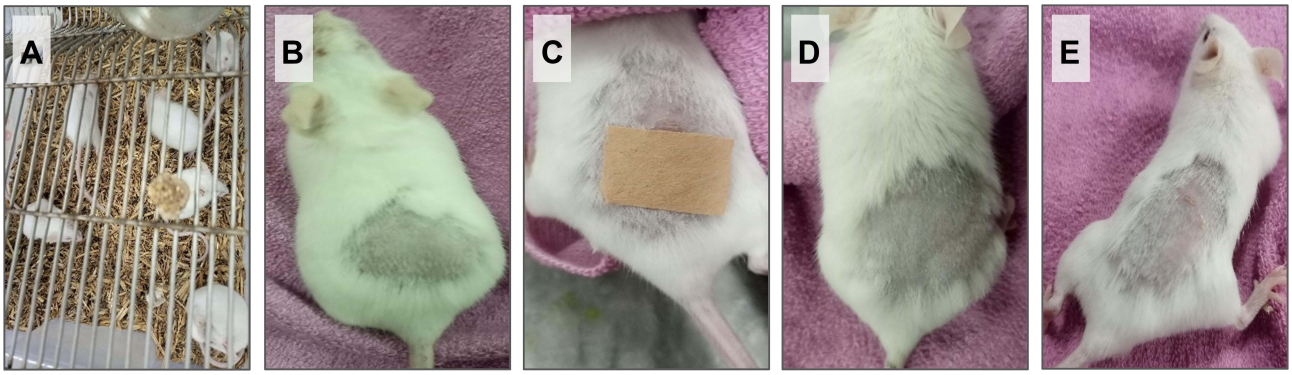

Figure 8 Irritation study on mice. (**A**) animals in the animal cage (**B**) animal skin shaved (**C**) film applied on the shaved skin (**D**) the skin after removal of the patch (**E**) control animal after treatment with formalin, irritation or redness on the skin can be seen.

Scanning Electron Microscopy (SEM)

The surface morphology of the transdermal PVA film with or without the HNTs was analyzed on SEM. The presence of HNTs increased the roughness of the film comparable with PVA without HNT (see Figure 7). The PVA film can be seen properly covered with the HNTs. The good bonding between PVA and HNTs enhances the mechanical stability of the composite. The nanotubes wrapped with the polymer also increase the stability of the film.[66] The absence of agglomeration or fractured surfaces on the film indicates a uniform distribution of the film components.

Skin Irritation Study

The transdermal films were applied to the mice and evaluated for skin irritation such as edema or erythema. A moderate erythema reaction was observed in control group mice (Figure 8). There was almost no skin irritation observed in the test group mice compared to the control group, and the films were found safe. The transdermal delivery systems containing propranolol HCl were observed non-irritant to the skin and suggested to be safe in other studies also.[67,68]

In silico Modeling and Simulation

The systemic absorption and disposition prediction for optimized propranolol HCl formulation (F6) was carried out using the TCAT® model. Contemplating the oral administration of 80 mg propranolol and to simulate the systemic disposition into individuals with an average weight of 75 kg as a comparison parameter, the three-compartmental model was selected with the help of the PKPlus® module.[69] Different formulations, pharmacokinetics, and physiological parameters are illustrated in Table 2. The mean pharmacokinetic parametric values (Table 7) for F6 were calculated as 32.113 ng/mL (C_{max}), 16.58 h (T_{max}), 942.34 ng/mL×h (AUC_t) and 1102.9 ng/mL×h (AUC_{inf}). After selecting different application areas and dosage strength, the model integrated pharmacokinetic parameters and TCAT® model for F6 using values of a dose of 20 mg and 9 cm^2 as the application surface area.

The predicted plasma concentration profiles after 80 mg oral and 20 mg transdermal administration of propranolol HCl are shown in Figure 9A. A similarity between bioavailability profiles can be readily observed from both the curves though having different dosage strengths. This may be explained by the fact that propranolol HCl undergoes more than

Table 7 Predicted Values of Pharmacokinetic Parameters for Transdermal Nanocomposite Film of Propranolol HCl

Parameter	Oral (80 mg)	TD (20 mg)	TD (20 mg × 4)
C_{max} (ng/mL)	36.653	32.113	51.959
T_{max} (h)	6.014	16.58	84.68
AUC $_{0 \rightarrow inf}$ (ng*hr/mL)	434.66	1102.9	4642.5
AUC $_{0 \rightarrow t}$ (ng*hr/mL)	405.33	942.34	3604.6

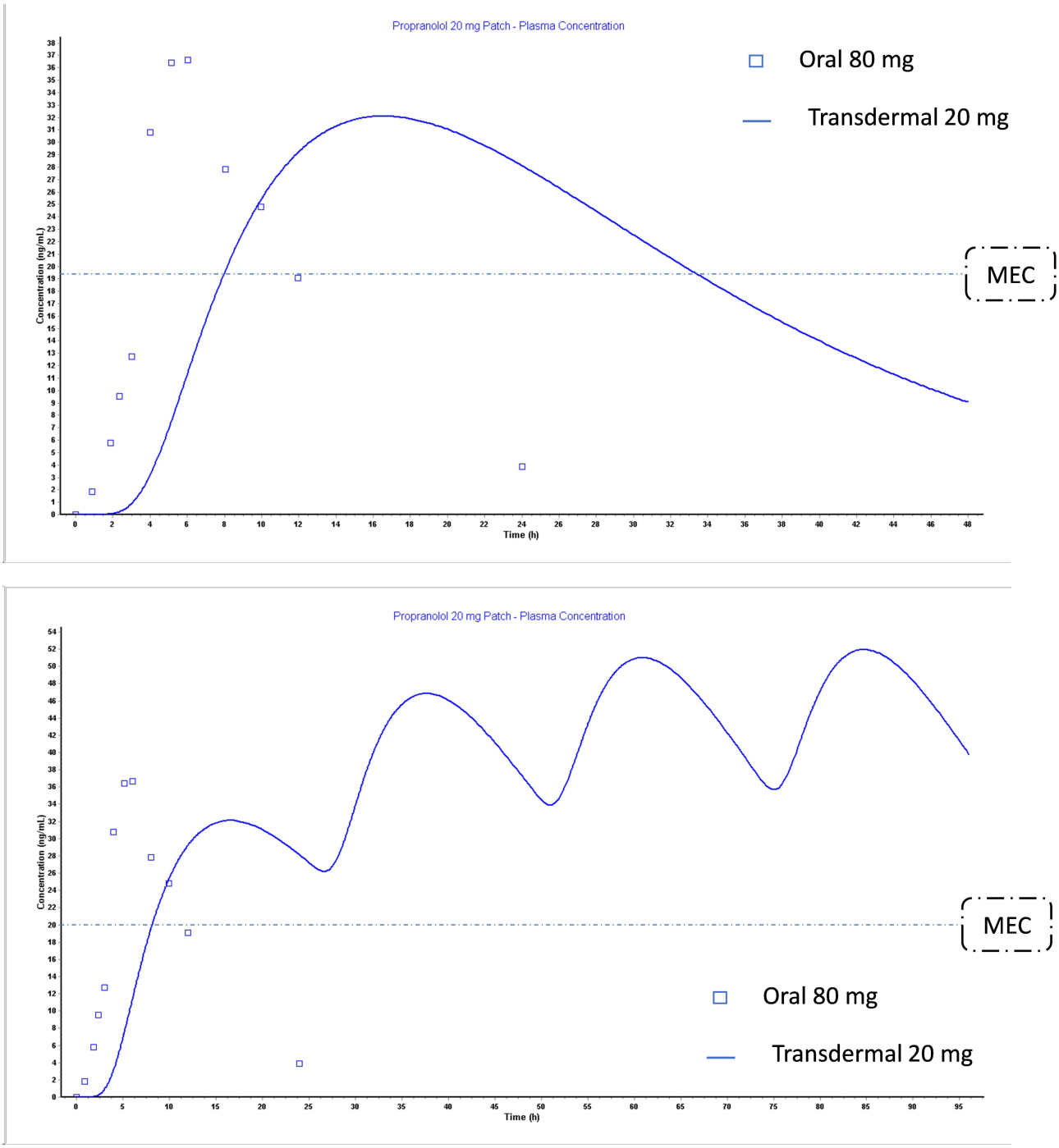

Figure 9 Plasma concentration–time profiles of (**A**) propranolol HCl oral 80 mg tablet formulation and simulated 20 mg transdermal nanocomposite propranolol film formulation F6 (**B**) propranolol HCl oral 80 mg tablet formulation and simulation of multiple doses (4 doses) of F6 using Gastroplus™ PBPK modeling software.

75% first-pass metabolism via the oral route.[18] A cumulative increase in the plasma concentration of propranolol administered by a transdermal route was a bit slower when compared with the oral route. However, it was found to be equal after 9 hours of transdermal application. However, continuous therapy with multiple dosing suggests that the plasma profile is maintained in the therapeutic window (see Figure 9B) and the plasma levels are retained above the minimum therapeutic concentration (20 ng/mL).[70]

This 20 mg dose of propranolol HCl, which is four-fold lesser than the oral route would suggest that the transdermal system embedded with halloysite nanotubes would be implicit in promoting drug diffusion across the skin compartments

Table 8 Drug Content, Dissolution and Permeation Performance of Transdermal Nanocomposite Kept at Room and Accelerated Temperature for 3 Months

	Period	Room Temperature (25°C ± 2°C and 60% RH ± 5%)	Accelerated Temperature (40°C ± 2°C and 75% RH ± 5%)
Drug content (%)	1 Week	96.371±0.220	96.294±0.605
Dissolution test (%)		79.829±0.780	79.191±2.331
Permeation test (μg/cm^2)		459.380±9.170	465.055±7.919
Drug content (%)	1.5 Months	96.242±0.311	95.852±0.433
Dissolution test (%)		78.280±0.245	81.708±0.583
Permeation test (μg/cm^2)		462.308±10.019	455.843±6.727
Drug content (%)	3 Months	96.138±0.428	95.567±0.518
Dissolution test (%)		80.289±1.164	79.739±1.036
Permeation test (μg/cm^2)		451.581±9.161	441.321±2.073

and effectively delivering therapeutic concentrations of propranolol HCl. This is an important feature of the transdermal route as the release kinetics, and cutaneous absorption can provide controlled plasma drug concentrations.[71] Based on the results obtained from in silico pharmacokinetic modeling, it is observed that the viability of halloysite nanotubes in the transdermal route as an alternative to oral administration for hypertension therapy diminishes hepatic first-pass load and possible adverse effects.

Stability Study

The stability study of the optimized transdermal film formulation (F6) was carried out at the room and at accelerated temperature. The physical characteristics, drug content, release, and permeation of the propranolol HCl were determined at different time intervals during the study, as shown in Table 8. The nanocomposite was observed to be satisfied physically, and no substantial change in the physical appearance was observed. The content of propranolol HCl was found to be 96.13 ± 0.42% at room temperature and 95.56 ± 0.51% at accelerated temperature. Although no significant difference in the drug content was observed, a slight decrease at higher temperatures might be due to the effect of certain environmental factors such as heat, moisture, and oxygen that could influence the stability of the drug and reduce the shelf life of the formulation.[72] Similarly, the permeation of the drug was observed to decrease after prolonged storage, especially at accelerated temperature. The permeation parameters were calculated, and it was revealed that the flux rate decreased (140.878 μg/cm^{2}h and 138.299 μg/cm^{2}h) while the lag time increased (0.363 hr and 0.370 hr) after 3 months of storage. The loss of permeation enhancers after prolonged storage might be responsible for the reduction in permeation of the drug substance through the barrier membrane.[72] The shelf life of propranolol HCl transdermal nanocomposite films was calculated and found to be 35.46 months at 28–30 °C and 19.66 months at 40–45 °C. Therefore, it can be proposed that the transdermal formulation should be stored at room temperature. The same has also been suggested for the propranolol HCl oral formulation.[73]

Conclusion

Halloysite nanotubes-based transdermal nanocomposite films of propranolol HCl with different ratios of HNTs were formulated and evaluated. The nanocomposite films have a satisfactory appearance and mechanical stability, insignificant variation in weight and thickness and sufficient drug content. It was revealed that the drug release from the formulation was controlled with the increase in HNTs, and the permeation was enhanced. The menthol 1% concentration also enhanced the permeation of propranolol HCl through the barrier membrane. The drug release was found following the Korsmeyer–Peppas model with an n value of less than 0.5, representing Fickian diffusion. The formulation F6, which

contained the 2:1 ratio of drug to HNTs, was selected as optimized due to a suitable release and permeation profile. The optimized formulation was considered safe and non-irritant to the skin. Moreover, the formulation was found mechanically stable, while the components were chemically non-reacting to the drug product, and the surface morphology revealed uniform distribution of HNTs in the composite. A maintained therapeutic window was also predicted from the in silico model. Furthermore, the formulation was found more stable at room temperature. Based on the data obtained, the HNTs could be a potential candidate for developing a transdermal drug delivery system, and the PVA/HNTs nanocomposite can be used for the design of a cost-effective and commercially viable transdermal drug delivery system with fewer regulatory challenges.

Disclosure

The authors report no conflicts of interest in this work.

References

1. Miller KJ. Transdermal product formulation development. In: Heather AE, Benson ACW, editors. *Transdermal and Topical Drug Delivery - Principles and Practice*. Firsted. Hoboken, New Jersey: John Wiley & Sons, Inc.; Vol. 1, 2012: 287.
2. Ita K. *Transdermal Drug Delivery - Concepts and Application*. Vol. 1. UK: Elsevier; 2020.
3. Chien YW. *Novel Drug Delivery Systems*. Seconded.Boca Raton, FL: CRC Press Taylor & Francis Group; Vol. 14, 1991.
4. Paudel KS, Milewski M, Swadley CL, Brogden NK, Ghosh P, Stinchcomb AL. Challenges and opportunities in dermal/transdermal delivery. *Ther Deliv*. 2010;1(1):109–131. doi:10.4155/tde.10.16
5. Liechty WB, Kryscio DR, Slaughter BV, Peppas NA. Polymers for drug delivery systems. *Annu Rev Chem Biomol Eng*. 2010;1:149–173. doi:10.1146/annurev-chembioeng-073009-100847
6. Setter OP, Segal E. Halloysite nanotubes–the nano-bio interface. *Nanoscale*. 2020;12(46):23444–23460. doi:10.1039/D0NR06820A
7. Fizir M, Dramou P, Dahiru NS, Ruya W, Huang T, He H. Halloysite nanotubes in analytical sciences and in drug delivery: a review. *Microchim Acta*. 2018;185(8):1–33. doi:10.1007/s00604-018-2908-1
8. Massaro M, Noto R, Riela S. Past, present and future perspectives on halloysite clay minerals. *Molecules*. 2020;25(20):4863. doi:10.3390/molecules25204863
9. Khatoon N, Chu MQ, Zhou CH. Nanoclay-based drug delivery systems and their therapeutic potentials. *J Mater Chem B*. 2020;8(33):7335–7351. doi:10.1039/D0TB01031F
10. Husain T, Shoaib MH, Ahmed FR, et al. Investigating halloysite nanotubes as a potential platform for oral modified delivery of different BCS class drugs: characterization, optimization, and evaluation of drug release kinetics. *Int J Nanomedicine*. 2021;16:1725-1741. doi:10.2147/IJN.S299261
11. Ahmed FR, Shoaib MH, Azhar M, et al. In-vitro assessment of cytotoxicity of halloysite nanotubes against HepG2, HCT116 and human peripheral blood lymphocytes. *Colloids Surf B Biointerfaces*. 2015;135:50–55. doi:10.1016/j.colsurfb.2015.07.021
12. Krejčová K, Deasy PB, Rabišková M. Optimization of diclofenac sodium profile from halloysite nanotubules. Ceska a Slovenska farmacie: casopis Ceske farmaceuticke spolecnosti a Slovenske farmaceuticke spolecnosti. *Ceska a Slovenska Farmacie*. 2013;62(2):71–77.
13. Ahmed FR, Shoaib MH, Yousuf RI, et al. Clay nanotubes as a novel multifunctional excipient for the development of directly compressible diclofenac potassium tablets in a SeDeM driven QbD environment. *Eur J Pharm Sci*. 2019;133:214–227. doi:10.1016/j.ejps.2019.03.028
14. Fakhruddin K, Hassan R, Khan MUA, et al. Halloysite nanotubes and halloysite-based composites for biomedical applications. *Arab J Chem*. 2021;14(9):103294. doi:10.1016/j.arabjc.2021.103294
15. Gaaz TS, Sulong AB, Akhtar MN, Kadhum AAH, Mohamad AB, Al-Amiery AA. Properties and applications of polyvinyl alcohol, halloysite nanotubes and their nanocomposites. *Molecules*. 2015;20(12):22833–22847. doi:10.3390/molecules201219884
16. Zhou WY, Guo B, Liu M, Liao R, Rabie AB, Jia D. Poly(vinyl alcohol)/halloysite nanotubes bionanocomposite films: properties and in vitro osteoblasts and fibroblasts response. *J Biomed Mater Res A*. 2010;93(4):1574–1587. doi:10.1002/jbm.a.32656
17. Al-Majed AA, Bakheit AHH, Abdel Aziz HA, Alajmi FM, AlRabiah H. Chapter six - propranolol. In: Brittain HG, editor. *Profiles of Drug Substances, Excipients and Related Methodology*. Vol. 42. Academic Press; 2017:287–338.
18. Calatayud-Pascual MA, Sebastian-Morelló M, Balaguer-Fernández C, Delgado-Charro MB, López-Castellano A, Merino V. Influence of chemical enhancers and iontophoresis on the in vitro transdermal permeation of propranolol: evaluation by dermatopharmacokinetics. *Pharmaceutics*. 2018;10(4):265. doi:10.3390/pharmaceutics10040265
19. National Center for Biotechnology Information. PubChem compound summary for CID 4946, propranolol; 2004. Available from: https://pubchem.ncbi.nlm.nih.gov/compound/Propranolol. Accessed March 14, 2021.
20. USP 35. 4462 propoxyphene/official monographs. United States pharmacopeial convention; 2011. Available from: http://www.drugfuture.com/Pharmacopoeia/usp35/PDF/4462-4462%20Propranolol%20Hydrochloride.pdf. Accessed July 27, 2022.
21. Percie du Sert N, Hurst V, Ahluwalia A, et al. The ARRIVE guidelines 2.0: updated guidelines for reporting animal research. *PLoS Biol*. 2020;18(7):e3000410. doi:10.1371/journal.pbio.3000410
22. Institute of Laboratory Animal Resources (US). National research council committee for the update of the guide for the C, use of Laboratory A. the national academies collection: reports funded by national institutes of health. In: *Guide for the Care and Use of Laboratory Animals*. Washington (DC): National Academies Press (US) Copyright ©; 2011.
23. Zhong B, Wang S, Dong H, et al. Halloysite tubes as nanocontainers for herbicide and its controlled release in biodegradable poly(vinyl alcohol)/starch film. *J Agric Food Chem*. 2017;65(48):10445–10451. doi:10.1021/acs.jafc.7b04220
24. Prabhu P, Shah S, Gundad S. Formulation development and investigation of domperidone transdermal patches. *Int J Pharm Investig*. 2011;1(4):240–246. doi:10.4103/2230-973X.93008

25. Al Hanbali OA, Khan HMS, Sarfraz M, Arafat M, Ijaz S, Hameed A. Transdermal patches: design and current approaches to painless drug delivery. *Acta Pharm*. 2019;69(2):197–215. doi:10.2478/acph-2019-0016
26. Mohd F, Bontha L, Bontha V, Vemula S. Formulation and evaluation of transdermal films of ondansetron hydrochloride. *MOJ Bioequiv Availab*. 2017;3(4):00039.
27. Arora P, Mukherjee B. Design, development, physicochemical, and in vitro and in vivo evaluation of transdermal patches containing diclofenac diethylammonium salt. *J Pharm Sci*. 2002;91(9):2076–2089. doi:10.1002/jps.10200
28. David SRN, Rajabalaya R, Zhia ES. Development and in vitro evaluation of self-adhesive matrix-type transdermal delivery system of ondansetron hydrochloride. *Trop J Pharma Res*. 2015;14(2):211–218. doi:10.4314/tjpr.v14i2.4
29. Amnuaikit C, Ikeuchi I, Ogawara K-I, Higaki K, Kimura T. Skin permeation of propranolol from polymeric film containing terpene enhancers for transdermal use. *Int J Pharm*. 2005;289(1–2):167–178. doi:10.1016/j.ijpharm.2004.11.007
30. Zhang Y, Huo M, Zhou J, et al. DDSolver: an add-in program for modeling and comparison of drug dissolution profiles. *AAPS J*. 2010;12(3):263–271. doi:10.1208/s12248-010-9185-1
31. Haney P, Herting K, Smith S. *Molecular Weight Cut-Off (Mwco) Specifications and Rates of Buffer Exchange With Slide-A-Lyzer Dialysis Devices and Snakeskin Dialysis Tubing*. Waltam: Protein Biology Resource Library, ThermoFisher Scientific; 2013.
32. Kelchen MN, Brogden NK. In vitro skin retention and drug permeation through intact and microneedle pretreated skin after application of propranolol loaded microemulsions. *Pharm Res*. 2018;35(12):1–12. doi:10.1007/s11095-018-2495-1
33. Ubaidulla U, Reddy MVS, Ruckmani K, Ahmad FJ, Khar RK. Transdermal therapeutic system of carvedilol: effect of hydrophilic and hydrophobic matrix on in vitro and in vivo characteristics. *AAPS Pharm Sci Tech*. 2007;8(1):E13–E20. doi:10.1208/pt0801002
34. Kunta JR, Goskonda VR, Brotherton HO, Khan MA, Reddy IK. Effect of menthol and related terpenes on the percutaneous absorption of propranolol across excised hairless mouse skin. *J Pharm Sci*. 1997;86(12):1369–1373.
35. Adrian Williams C. Topical and transdermal drug delivery. In: Taylor KMG, editor. *Aulton's Pharmaceutics - the Design and Manufacture of Medicine*. Fifthed. UK: Elsevier; Vol. 1, 2018: 715–738.
36. Council NR Guide for the care and use of laboratory animals; 2010.
37. Singh A, Bali A. Formulation and characterization of transdermal patches for controlled delivery of duloxetine hydrochloride. *J Anal Sci Technol*. 2016;7(1):1–13. doi:10.1186/s40543-016-0105-6
38. Vlasses PH, Ribeiro L, Rotmensch HH, et al. Initial evaluation of transdermal timolol: serum concentrations and beta-blockade. *J Cardiovasc Pharmacol*. 1985;7(2):245–250. doi:10.1097/00005344-198503000-00006
39. PubChem compound summary for CID 62882, propranolol hydrochloride; 2022. Available from: https://pubchem.ncbi.nlm.nih.gov/compound/Propranolol-hydrochloride. Accessed July 27, 2022.
40. Drug Bank. Propranolol; 2022. Available from: https://go.drugbank.com/drugs/DB00571. Accessed July 27, 2022.
41. Taylor E, Turner P. The distribution of propranolol, pindolol and atenolol between human erythrocytes and plasma. *Br J Clin Pharmacol*. 1981;12(4):543–548. doi:10.1111/j.1365-2125.1981.tb01263.x
42. Kalam MN, Rasool MF, Alqahtani F, Imran I, Rehman AU, Ahmed N. Development and evaluation of a physiologically based pharmacokinetic drug-disease model of propranolol for suggesting model informed dosing in liver cirrhosis patients. *Drug Des Devel Ther*. 2021;15:1195–1211. doi:10.2147/DDDT.S297981
43. Puri A, Bhattaccharjee SA, Zhang W, et al. Development of a transdermal delivery system for tenofovir alafenamide, a prodrug of tenofovir with potent antiviral activity against HIV and HBV. *Pharmaceutics*. 2019;11(4):173. doi:10.3390/pharmaceutics11040173
44. Nair RS, Ling TN, Shukkoor MSA, Manickam B. Matrix type transdermal patches of captopril: ex vivo permeation studies through excised rat skin. *J Pharm Res*. 2013;6(7):774–779. doi:10.1016/j.jopr.2013.07.003
45. Abdullah Z, Dong Y. Biodegradable and water resistant Poly(vinyl) Alcohol (PVA)/Starch (ST)/Glycerol (GL)/Halloysite Nanotube (HNT) nanocomposite films for sustainable food packaging. *Front Mater*. 2019;6:58. doi:10.3389/fmats.2019.00058
46. Mutalik S, Udupa N. Glibenclamide transdermal patches: physicochemical, pharmacodynamic, and pharmacokinetic evaluations. *J Pharm Sci*. 2004;93(6):1577–1594. doi:10.1002/jps.20058
47. Abdouss M, Radgoudarzi N, Mohebali A, Kowsari E, Koosha M, Li T. Fabrication of bio-nanocomposite based on hnt-methionine for controlled release of phenytoin. *Polymers*. 2021;13(15):2576. doi:10.3390/polym13152576
48. Al-Sahaf Z, Raimi-Abraham B, Licciardi M, de Mohac LM. Influence of Polyvinyl Alcohol (PVA) on PVA-Poly-N-hydroxyethyl-aspartamide (PVA-PHEA) microcrystalline solid dispersion films. *AAPS Pharm Sci Tech*. 2020;21(7):267. doi:10.1208/s12249-020-01811-z
49. Levis SR, Deasy PB. Use of coated microtubular halloysite for the sustained release of diltiazem hydrochloride and propranolol hydrochloride. *Int J Pharm*. 2003;253(1):145–157. doi:10.1016/S0378-5173(02)00702-0
50. Rohaľová S, Guman M, Wolaschka T. Transdermal patches for delivery of beta-blockers. *Eur Pharm J*. 2021;68(1):80–83. doi:10.2478/afpuc-2021-0007
51. Swapna V, Suresh K, Saranya V, Rahana M, Stephen R, Stephen R. Thermal properties of poly (vinyl alcohol)(PVA)/halloysite nanotubes reinforced nanocomposites. *Int J Plast Technol*. 2015;19(1):124–136. doi:10.1007/s12588-015-9106-3
52. Costa P, Sousa Lobo JM. Modeling and comparison of dissolution profiles. *Eur J Pharm Sci*. 2001;13(2):123–133. doi:10.1016/S0928-0987(01)00095-1
53. Mohebali A, Abdouss M, Afshar Taromi F. Fabrication of biocompatible antibacterial nanowafers based on HNT/PVA nanocomposites loaded with minocycline for burn wound dressing. *Mater Sci Eng*. 2020;110:110685. doi:10.1016/j.msec.2020.110685
54. Arafa K, Shamma RN, El-Gazayerly ON, El-Sherbiny IM. Facile development, characterization, and optimization of new metformin-loaded nanocarrier system for efficient colon cancer adjunct therapy. *Drug Dev Ind Pharm*. 2018;44(7):1158–1170. doi:10.1080/03639045.2018.1438463
55. Jeevan R, Venkat R, Khan MA, Brotherton HO, Reddy IK. Effect of menthol and related terpenes on the percutaneous absorption of propranolol across excised hairless mouse skin. *J Pharm Sci*. 1997;86(12):1369–1373.
56. Krishna R, Pandit J. Carboxymethylcellulose-sodium based transdermal drug delivery system for propranolol. *J Pharm Pharmacol*. 1996;48(4):367–370. doi:10.1111/j.2042-7158.1996.tb05934.x
57. Díaz-Torres R. Transdermal nanocarriers. In: Escobar-Chávez JJ, editor. *Current Technologies to Increase the Transdermal Delivery of Drugs*. Firsted. USA: Bentham Science Publishers; Vol. 1, 2010: 121.

58. USP. Propranolol hydrochloride extended release capsules. The United States Pharmacopeial Convention; 2020. Available from: https://www.uspnf.com/sites/default/files/usp_pdf/EN/USPNF/revisions/propranolol-hcl-erc-pending-nitr-20200327.pdf. Accessed July 27, 2022.
59. Srikanth MV, Rao NS, Sunil SA, Ram BJ, Kolapalli VRM. Statistical design and evaluation of a propranolol HCl gastric floating tablet. *Acta Pharm Sin B*. 2012;2(1):60–69. doi:10.1016/j.apsb.2011.12.008
60. Gaaz TS, Sulong AB, Kadhum AAH, Al-Amiery AA, Nassir MH, Jaaz AH. The impact of halloysite on the thermo-mechanical properties of polymer composites. *Molecules*. 2017;22(5):838. doi:10.3390/molecules22050838
61. Joussein E, Petit S, Churchman J, Theng B, Righi D, Delvaux BJCM. Halloysite clay minerals—a review. *Clay Miner*. 2005;40(4):383–426.
62. Trivedi MK, Patil S, Mishra R, Jana SJMP, Research OP. Structural and physical properties of biofield treated thymol and menthol. *Mol Pharm Org Process Res*. 2015;3(2):1000127.
63. Macêdo R, Gomes Do Nascimento T, Veras JJJ. Compatibility and stability studies of propranolol hydrochloride binary mixtures and tablets for TG and DSC-photovisual. *J Therm Anal Calorim*. 2002;67(2):483–489. doi:10.1023/A:1013901332759
64. Do Nascimento DC, da Silva MGC, Vieira MGAJJo ML. Adsorption of propranolol hydrochloride from aqueous solutions onto thermally treated bentonite clay: a complete batch system evaluation. *J Mol Liq*. 2021;337:116442. doi:10.1016/j.molliq.2021.116442
65. Del Mar Orta M, Martín J, Medina-Carrasco S, Santos JL, Aparicio I, Alonso EJACS. Adsorption of propranolol onto montmorillonite: kinetic, isotherm and pH studies. *Appl Clay Sci*. 2019;173:107–114. doi:10.1016/j.clay.2019.03.015
66. Azmi S, Razak SIA, Abdul Kadir MR, et al. Reinforcement of poly (vinyl alcohol) hydrogel with halloysite nanotubes as potential biomedical materials. *Soft Mater*. 2017;15(1):45–54. doi:10.1080/1539445X.2016.1242500
67. Sharan G, Dey K, Das S, Kumar V. Effect of various permeation enhancers on propranolol hydrochloride formulated patches. *Int J Pharmacy Pharm Sci*. 2010;2(2):21–31.
68. Verma P, Iyer SS. Transdermal delivery of propranolol using mixed grades of Eudragit: design and in vitro and in vivo evaluation. *Drug Dev Ind Pharm*. 2000;26(4):471–476. doi:10.1081/DDC-100101257
69. van der Heijden JT, Krenning EP, van Toor H, Hennemann G, Docter R. Three-compartmental analysis of effects of D-propranolol on thyroid hormone kinetics. *Am J Physiol*. 1988;255(1 Pt 1):E80–86. doi:10.1152/ajpendo.1988.255.1.E80
70. Mansur A, Avakian S, Paula R, Donzella H, Santos S, Ramires J. Pharmacokinetics and pharmacodynamics of propranolol in hypertensive patients after sublingual administration: systemic availability. *Braz J Med Biol*. 1998;31(5):691–696. doi:10.1590/S0100-879X1998000500014
71. Yamamoto S, Karashima M, Arai Y, Tohyama K, Amano N. Prediction of human pharmacokinetic profile after transdermal drug application using excised human skin. *J Pharm Sci*. 2017;106(9):2787–2794. doi:10.1016/j.xphs.2017.03.003
72. Benecke AG, Kinne DJ, Wnuk AJ. *Storage-Stable Transdermal Patch*. Google Patents; 1991.
73. FDA. Inderal® (propranolol hydrochloride) tablets, reference ID: 2919389. Available from: https://www.accessdata.fda.gov/drugsatfda_docs/label/2011/016418s080,016762s017,017683s008lbl.pdf. Accessed March 14, 2021.